Nuclear Inst. and Methods in Physics Research, A 1040 (2022) 167182

Contents lists available at ScienceDirect

Nuclear Inst. and Methods in Physics Research, A

journal homepage: www.elsevier.com/locate/nima

High-temperature performance of solid-state sensors up to 500 °C

C. Weiss [a,b,*], J. Wilson [c,d], G. Tiebel [c,d], P. Steinegger [c,d], E. Griesmayer [a,b], H. Frais-Kölbl [e], R. Dressler [c], M. Camarda [f], M. del Mar Carulla Areste [c]

[a] TU Wien, Atominstitut, Vienna, Austria
[b] CIVIDEC Instrumentation GmbH, Vienna, Austria
[c] Paul Scherrer Institut, Villigen PSI, Switzerland
[d] ETH Zürich, Zürich, Switzerland
[e] University of Applied Sciences, Wiener Neustadt, Austria
[f] SenSiC GmbH, Park InnovAARE, Villigen, Switzerland

ARTICLE INFO

Keywords:
sCVD diamond sensor
4H-siC sensor
Particle spectroscopy
High-temperature

ABSTRACT

The applicabilities of single-crystal chemical vapour deposition diamond sensors and 4H-SiC diodes for particle spectroscopy in high-temperature environments are investigated. The spectroscopic performance of the sensor materials is measured as function of temperature, from room temperature to 500 °C. Previously published measurements showed a stable spectroscopic response of sCVD diamond sensors up to 200 °C. In this follow-up experiment, the temperature range was extended up to 500 °C for sCVD diamond as well as 4H-SiC sensors.

1. Introduction

The applicability of single-crystal Chemical Vapour Deposition (sCVD) diamond sensors for particle spectroscopy from ambient temperatures up to 200 °C was reported in Ref. [1]. Among other fields, the motivation to increase the temperature range even further originates in the chemical characterization of transactinide elements using gas-chromatography. Higher detector and thus stationary surface temperatures will considerably expand the range of accessible chemical elements and their compounds, see Ref. [2] for details.

The charge carrier properties of sCVD diamond were investigated for low temperatures in Ref. [3]. In this work, first results for temperatures up to 500 °C are presented for sCVD diamond as well as a 4H-SiC sensor.

2. Experimental setup

Two sensors were used in the measurements:

1. sCVD diamond: 4.5 mm × 4.5 mm × 140 μm, metallized with 4 mm × 4 mm Ti-Pt-Au-electrodes.
2. 4H-SiC: 4.5 mm × 4.5 mm crystal with approx. 30 μm depletion zone and a 4 mm × 4 mm Ti-Al-Ni electrode (front side) and a pure Ni-electrode (rear side).

The measurements were performed under vacuum at $\leq 10^{-6}$ mbar with an ^{241}Am α-source. The sensors were installed in a three-layered ceramic printed circuit board (PCB) structure, identical to the setup presented in Ref. [1]. The electric contacting was established using a Au-plated stainless-steel spring, which also mechanically clamped the sensor inside the carrier structure. A schematics of the experimental setup is shown in Fig. 1.

The detector assembly was enclosed in a Cu heat spreader, featuring two resistive heating cartridges. The heating cartridges were continuously powered to steadily increase the temperature over the course of the experiment. A Type-K thermocouple was inserted in the ceramic carrier to measure the sensor temperature T. The tip of the thermocouple was 3 mm away from the edge of the sensor. A Lutron thermometer recorded T over time. The systematic uncertainty is estimated as $\Delta T = \pm 10$ °C for this experimental setup and the heat rate. At lowest and highest temperatures the experimental setup was kept at temperature for longer and the systematic uncertainty of the measurement is reduced.

Electronics. The sensor signals are read out via the ground electrode of the sensor (see circuit diagram in Fig. 2). The bias voltage for both sensors was set to HV = −150 V in all experiments. The α-particles entered the sensors through the bias electrode and have a penetration depth of 15 μm in diamond and 19 μm in SiC. Thus, the presented results correspond to electron-drift (e^--drift) dominated signals for the diamond sensor, see Ref. [4] for details. The bias voltage was supplied by a Keithley 2470 source meter, which was also used to measure the bias current I_{bias} of the sensors. As I_{bias} varied over 4 orders of magnitude, the Keithley 2470 was used in autoscale mode.

Two different amplifier types were used:

* Corresponding author at: TU Wien, Atominstitut, Vienna, Austria.
E-mail address: christina.weiss@cividec.at (C. Weiss).

https://doi.org/10.1016/j.nima.2022.167182
Received 17 March 2022; Received in revised form 20 June 2022; Accepted 24 June 2022
Available online 12 July 2022

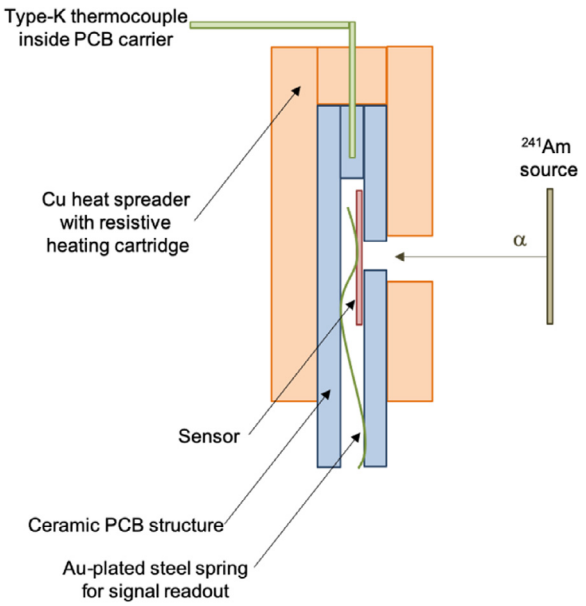

Fig. 1. Schematic of the experimental setup as installed inside the vacuum chamber.

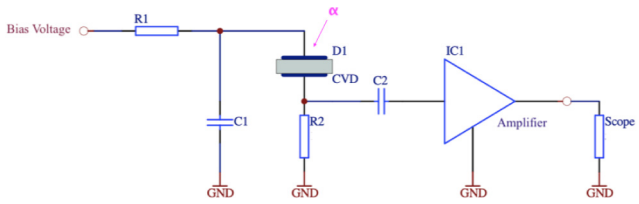

Fig. 2. Circuit diagram for the measurement setup. The α-particles entered the sensors through the bias electrode and the signals were read out via the ground electrode of the sensors.

(1) CIVIDEC C2-TCT Broadband Amplifier, 2 GHz, 40 dB: used for Transient-Current-Technique (TCT) measurements. The FWHM of TCT signals is equivalent to the drift time of the charge carriers in the sensor. The area of the TCT signals represents the collected charge Q.

(2) CIVIDEC Cx-L Spectroscopic Amplifier: used to precisely measure the charge yield as function of T. This charge sensitive amplifier, with a peaking time of 100 ns and a gain of A = 14.0 mV/fC, provides a Gaussian output pulse with FWHM = 180 ns. The amplitude of the output pulses corresponds to the collected charge.

Data analysis and synchronization. Each signal was recorded with a LeCroy WaveRunner 640Zi, 4 GHz oscilloscope, 40 GS/s, and analyzed offline for the signal amplitude h, the full width at half maximum FWHM and the area a, including a proper offset compensation. The standard deviation of the baseline was measured to study the impact of temperature on the noise contribution of the sensors. The area of the TCT-signals a_{TCT} was converted to the collected charge Q_{TCT} by using the electronically calibrated input impedance of Z_{in} = 55 Ω and the gain of the C2-TCT amplifier A_{TCT} = 156:

$$Q_{TCT} = a_{TCT}/(Z_{in} \cdot A_{TCT}) \quad (1)$$

The pulse amplitude h in the case of the spectroscopic Cx-L amplifier was converted to the collected charge Q by dividing it by the gain of the amplifier A = 14.0 mV/fC.

$$Q = h/A \quad (2)$$

The signal properties were stored together with the corresponding time stamp and synchronized with the results of the measurements of T and I_{bias}. One data matrix was compiled in this way for each measurement. Finally, the data was averaged over 2 °C intervals and the mean value μ and standard deviation σ were evaluated for the respective signal properties. The number of recorded signal traces per temperature interval for each of the experimental campaigns is shown in Fig. 3, to give an indication on the available statistics and on the heat rate.

Data was taken both, during heating up and cooling down of the sensors. In this paper, measurements during heating up are presented for reasons of consistency.

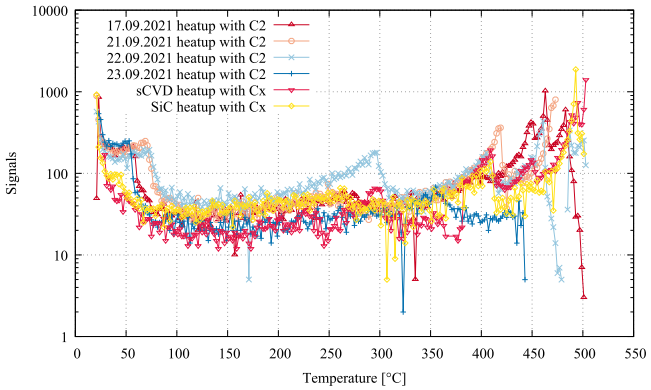

Fig. 3. Number of recorded signals per temperature interval for all experimental campaigns published in this paper.

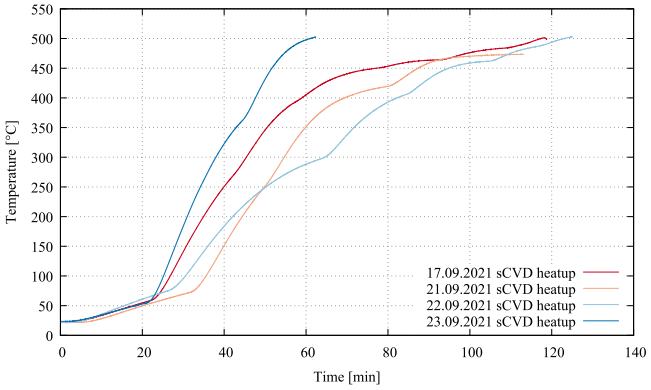

Fig. 4. Temperature as function of time for the 4 independent TCT measurement campaigns with the sCVD diamond sensor.

3. Results

3.1. TCT measurements with sCVD diamond

Four independent measurement campaigns were performed with the sCVD diamond sensor and the C2-TCT Broadband Amplifier. The corresponding heating progressions are shown in Fig. 4. The experimental setup was cooled down to room temperature between the campaigns with the vacuum maintained during all herein presented measurements. The FWHM of the TCT signals as function of T is shown in Fig. 5. The shape of the obtained distribution is fully reproducible between measurements. The progression of the FWHM values peaks at 220 °C and drops thereafter to a minimum at 260 °C from where it increases linearly up to 500 °C. The increase in e^--drift time for $T \leq 200$ °C is consistent with the results in Ref. [1], considering the different sensor thicknesses. The amplitude distribution, as recorded during the TCT-measurements, is shown in Fig. 6. The reduction of amplitude for $T < 220$ °C is consistent with the increase of FWHM, as their product corresponds to the collected charge.

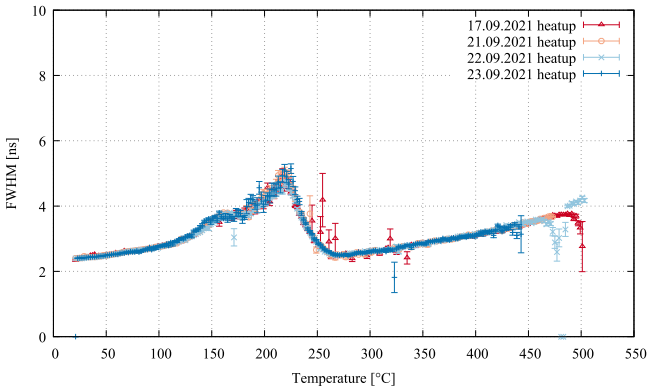

Fig. 5. FWHM of TCT-signals as function of T for the 140 µm thick sCVD diamond sensor measuring 5.5 MeV α-particles. An overall increase in e^--drift time with a systematic non-linearity for $T < 260$ °C is observed.

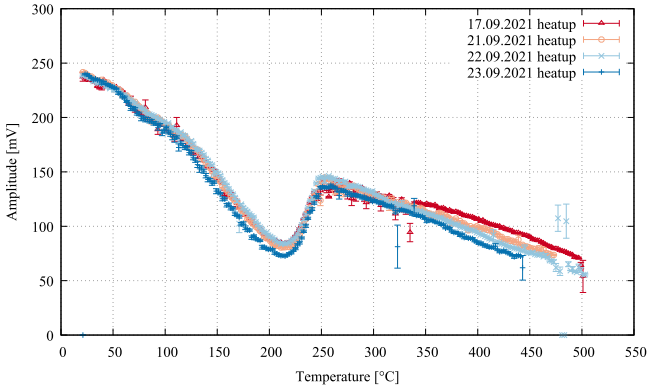

Fig. 6. Amplitudes of α-particle-induced TCT-signals as function of T for the sCVD diamond sensor. The overall decrease of amplitude and the non-linearity for $T < 260$ °C matches the characteristic of the signal FWHM.

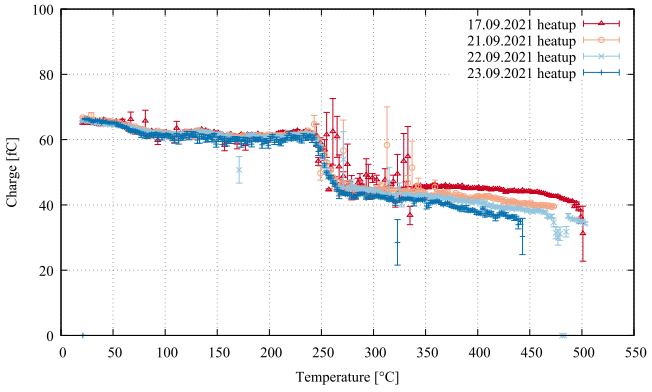

Fig. 7. Measured charge Q as function of T for the TCT-measurement campaigns with the sCVD diamond sensor. The areas of the TCT-signals were converted to Q using Eq. (1).

The measured charge as function of T is shown in Fig. 7. The distribution is constant up to 250 °C, where an immediate drop by about 30% occurs. Above this temperature threshold, a slight decrease of the measured charge with increasing temperature is observed. The four subsequent measurement campaigns show reduced amplitudes and charge levels in the range 320–500 °C.

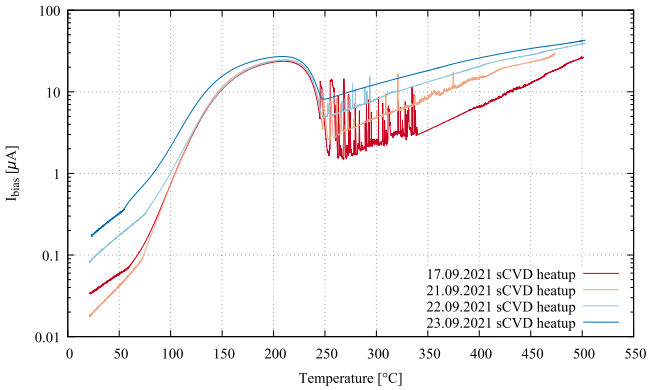

Fig. 8. Measured bias current as function of T for the sCVD diamond sensor. An overall exponential increase with a characteristic shoulder for $T < 250$ °C is observed. The peak structures are likely measurement artefacts caused by the autoscale function of the electrometer.

3.2. Bias current and noise measurement

During the TCT campaigns, the bias current I_{bias} and the baseline noise of the sCVD diamond sensor were measured as characteristic sensor parameters. The noise level remained constant as function of temperature in the full temperature range up to 500 °C. Meanwhile, an overall increase of I_{bias} with temperature T is observed (see Fig. 8) including a reproducible shoulder for $T < 250$ °C. An overall exponential increase of I_{bias} between heating cycles is observed. The peak structures are not systematic and are likely measurement artefacts from the autoscale function of the used source meter.

3.3. Spectroscopic measurements

The charge yield Q as function of T was measured in separate measurement campaigns for the sCVD diamond and 4H-SiC sensor using the spectroscopic measurement setup with the Cx-L amplifier. For each sensor one run is available to date.

sCVD diamond. The collected charge as function of T for the sCVD diamond sensor is shown in Fig. 9. The distribution is constant before a sudden dip is observed around $T = 260$ °C. Measurements performed beyond this temperature up to 500 °C revealed a slight downward trend of the collected charge. The measured charge at room temperature is (62.5 ± 0.4) fC, which converts to an electron–hole-pair creation energy in sCVD diamond of $E_{sCVD} = 13.6 \pm 0.1$ eV/eh-pair. This is in good agreement with the published value of 13 eV/eh-pair according to Ref [5]. At 500 °. C the charge yield dropped to about 83% of the value measured at room temperature.

4H-SiC. The measured charge Q as function of T for the 4H-SiC sensor is shown in Fig. 10. The charge yield is constant up to $T = 350$ °C. Beyond this temperature the collected charge decreases with increasing temperature. The measured charge at room temperature is 92.9 ± 0.6 fC, which converts to an electron–hole-pair creation energy in 4H-SiC of $E_{SiC} = 9.1 \pm 0.1$ eV/eh-pair, which is close to the published value of 7.8 eV/eh-pair in Ref. [5]. At 500 °C about 30% of the initial charge was measured compared to room temperature.

4. Conclusion

Measurements of a sCVD diamond and a 4H-SiC sensor from room temperature up to 500 °C are presented.

The spectroscopic measurement with the sCVD diamond sensor shows a constant charge response up to 250 °C and a 17% charge yield reduction at 500 °C.

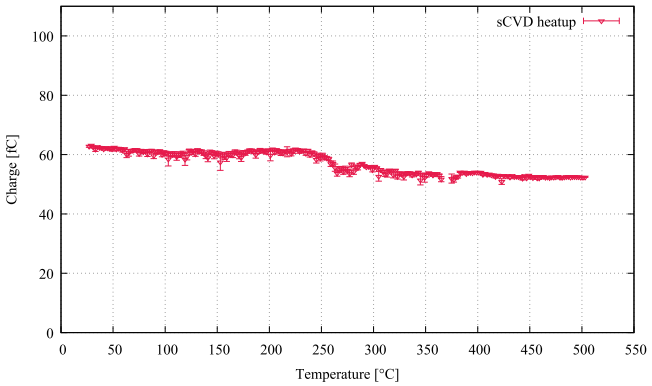

Fig. 9. Charge yield as function of T from the spectroscopic measurement of the 140 µm thick sCVD diamond sensor. A drop is observed around $T = 260$ °C. The charge yield at 500 °C is about 83%.

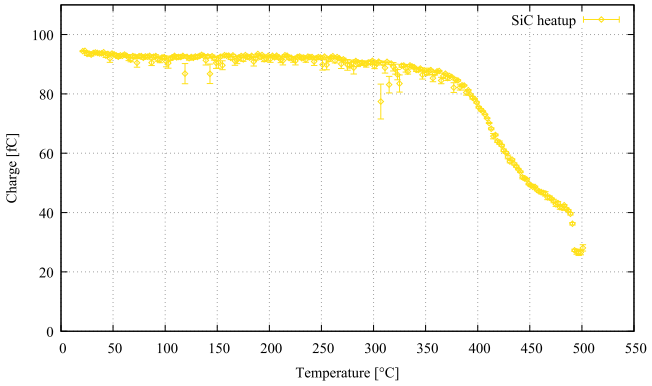

Fig. 10. Charge yield as function of T from the spectroscopic measurement of the 4H-SiC sensor. From 370 °C onwards, the charge yield drops by approximately 70% up to 500 °C.

The TCT-measurements of the sCVD diamond sensor show an increase of the e^--drift time in combination with a reduction of the signal amplitude, resulting in a relatively constant charge yield. Considering the different sensor thicknesses, these observations agree with previously published results up to 200 °C in Ref. [1]. For $T < 260$ °C a characteristic non-linearity is observed in the progression of drift times with temperature. Correspondingly, the dark current for sCVD diamond increases exponentially and likewise shows a shoulder when ramping up the temperature. As it is the case for the drift times, this shoulder does not appear when ramping down the temperature. The noise level of the sCVD diamond sensor remained constant across the full temperature range.

This study provides first insights into the charge response as function of temperature for 4H-SiC sensors up to 500 °C. The charge yield for 5.5 MeV α-particles at room temperature was determined to be 92.9 fC. The collected charge is constant up to 350 °C and shows a significant decrease of approximately 70% at 500 °C. This decrease of charge yield might be caused by a substantial increase of the e^--drift time with temperature, which was indicatively observed, and will be subject to further measurements.

5. Outlook

The presented results in this paper are observations from an ongoing research campaign, which aims to systematically investigate the high-temperature performance of sCVD diamond and 4H-SiC sensors for particle spectroscopy. The presented observations indicate that the time constants of heating up and cooling down influence the experimental results. Further spectroscopic measurement campaigns with varying heating rates are planned with both sensors, employing a parallel measurement of I_{bias} and the baseline noise. Aside of the generally demanding task of providing reliable electrical connections at high temperatures, further improvements concern a ceramic PCB heating structure with internal signal tracks. This will prevent metal deposits on otherwise insulating gaps on the PCB and thus, it will allow for generally longer heating cycles.

Additional TCT and spectroscopic measurements are planned with the sCVD diamond sensor for h^+-drift dominated signals.

TCT measurements for 4H-SiC sensors are planned, with larger depletions zones of > 100 µm.

Declaration of competing interest

The authors declare that they have no known competing financial interests or personal relationships that could have appeared to influence the work reported in this paper.

Acknowledgements

The authors want to thank Dominik Herrmann from PSI for his contributions to the experimental setup, especially the high-temperature-compatible steel spring.

This work received funding by SNSF, Switzerland under grant 200020_196981/1 and was supported by CIVIDEC Instrumentation GmbH, Austria and SenSiC GmbH, Switzerland.

References

[1] B. Kraus, P. Steinegger, N.V. Aksenov, R. Dressler, R. Eichler, E. Griesmayer, D. Herrmann, A. Türler, C. Weiss, Charge carrier properties of single-crystal CVD diamond up to 473 K, NIMA 989 (164947) (2021).

[2] P. Steinegger, M. Asai, R. Dressler, R. Eichler, Y. Kaneya, A. Mitsukai, Y. Nagame, D. Piguet, T.K. Sato, M. Schädel, S. Takeda, A. Toyoshima, K. Tsukada, A. Türler, A. Vascon, Vacuum chromatography of Tl and SiO_2 at the single-atom level, J. Phys. Chem. C 120 (13) (2016) 7122–7132, http://dx.doi.org/10.1021/acs.jpcc.5b12033.

[3] H. Jansen, Chemical Vapour Deposition Diamond: Charge Carrier Movement at Low Temperatures and Use in Time-Critical Applications (Ph.D. thesis), Rheinischen Friedrich-Wilhelms-Universität, Bonn, Germany, 2013.

[4] H. Pernegger, S. Roe, P. Weilhammer, V. Eremin, H. Frais-Kölbl, E. Griesmayer, H. Kagan, S. Schnetzer, R. Stone, W. Trischuk, D. Twitchen, A. Whitehead, Charge-carrier properties in synthetic single-crystal diamond measured with the transient-current technique, J. Appl. Phys. 97 (073704) (2005).

[5] P. Sellin, J. Vaitkus, New materials for radiation hard semiconductor detectors, 2005, CERN (23/03/2005 2005).